



THERMOPHYSICAL BEHAVIOURS OF P/M DISTALOY AE ALLOYS AT TEMPERATURE RANGE OF 0-600⁰C

Ayşe Nur ACAR¹, AbdulKadir EKŞİ², Ahmet EKİCİBİL³

¹Cukurova University, Ceyhan Engineering Faculty, Mechanical Engineering Department, , Adana,

²Cukurova University, Engineering Faculty, Mechanical Engineering Department, Adana,

³Cukurova University, Sciences and Letters Faculty, Physics Department, Adana,

Email: anacar@cu.edu.tr

Abstract

In this study, the thermophysical properties (specific heat capacity, enthalpy) of distaloy AE alloys have been investigated. Distaloy AE alloys were prepared by powder metallurgy method applying conventional pressing technique and heat treatment under N₂ atmosphere. Thermophysical properties of these alloys have been investigated at temperature ranging from 0 to 600 °C via heat flux type Differential Scanning Calorimeter (DSC) with 20 °C/min of heating rate, 50mL/min of gas flow and under N₂ atmosphere. These results supported with SEM images, EDS spectrums and XRD patterns of alloys.

Keywords: Distaloy AE, Powder metallurgy, Specific heat capacity, Enthalpy, Surface characterization

1.Introduction

Thermophysical properties such as specific heat capacity, enthalpy, *etc.*, of alloys can be changed by temperature without changing their chemical compositions. Specific heat capacity is referred as necessary heat amount that is increased temperature of one gram alloy by one degree, and enthalpy is internal energy of alloys [1-4]. Specific heat capacity and enthalpy are calculated with following Equations (1) and (2) [2, 4];

$$c_p = c_0 + c_1T + c_2T^2 + c_3T^{-3} \quad (1)$$

$$\Delta H = \int c_p dT \quad (2)$$

From Equations (1) and (2); c_0 , c_1 , c_2 , c_3 are coefficients of specific heat capacities of alloys, T is temperature. c_p and ΔH are symbolized as specific heat capacity and enthalpy, respectively [2,4]. In this study, distaloy AE alloy powder that

is diffusion bonded alloy type has utilized. This powder involves Fe, Ni and Mo alloying elements. This alloy has high strengthening structure and also high compatibility owing to their metallurgical bonding that is occurred among Fe-matrix and alloying elements dispersed into the Fe matrix. Production method plays important a role on the strengthening structure of alloy [5-9]. Powder metallurgy method, which is one of production methods of alloys, provides high strengthening structure due to consist of compacting and densification of powder/powder mixtures. This end-product may have denser structure [10-16]. In this study; specific heat capacity and enthalpy of these alloys prepared by powder metallurgy method have been investigated. The effects of pressure effect on these properties have been determined.

2. Material and Method

The chemical composition of Distaloy AE powder that is obtained from Höganäs in Sweden involves 0.01 of C%, 4.00 of Ni%, 1,5 of %Cu, 0.50 of Mo% and Fe in balance. In Figure 1; the SEM image of particle shape of this powder is observed. Particle shape of this powder has irregular shape and this irregular shaped powder provides compatibility.

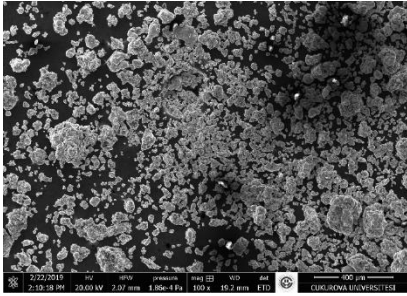


Figure 1. The SEM image of Distaloy AE powder

Prepared each of 37 g distaloy AE powder mixed with lubricant was placed into (10×15×70)mm prismatic mold, placed powder mixture pressed on the 400 and 600 MPa pressures using conventional pressing technique. After pressed green distaloy AE samples annealed at 600 and 900 °C temperatures for 30 min due to debind and provide uniform temperature distribution [17-19], annealed samples sintered at 1200°C temperature for 2 hour, after then, cooled to room temperature in furnace. Sintering stage occurred under N₂ atmosphere, heating and cooling rate were chosen as 5°C/min. Thermophysical properties (specific heat capacity, enthalpy) of these sintered distaloy AE samples have been examined at range from 0°C to 600°C using Differential Scanning Calorimeter (DSC) with 20 °C/min of heating rate, 50mL/min of gas flow and applied under N₂ atmosphere and also the specific heat capacity and enthalpy measurements of these samples supported by SEM images by FEI Quanta 650 Field Emission SEM device; EDS spectrums, which is subsidiary SEM device, and crystal structures of these samples characterized using PANalytical Empyrean XRD device ($\lambda=1.54\text{\AA}$).

3. Results and Discussions

In Figure 2; the specific heat capacity and enthalpy-temperature curves of distaloy AE samples prepared on 400 and 600 MPa pressures are seen and in Table 1. and 2, specific heat capacity and enthalpy values of these samples are given with fitted c_p and ΔH values and errors of percentages.

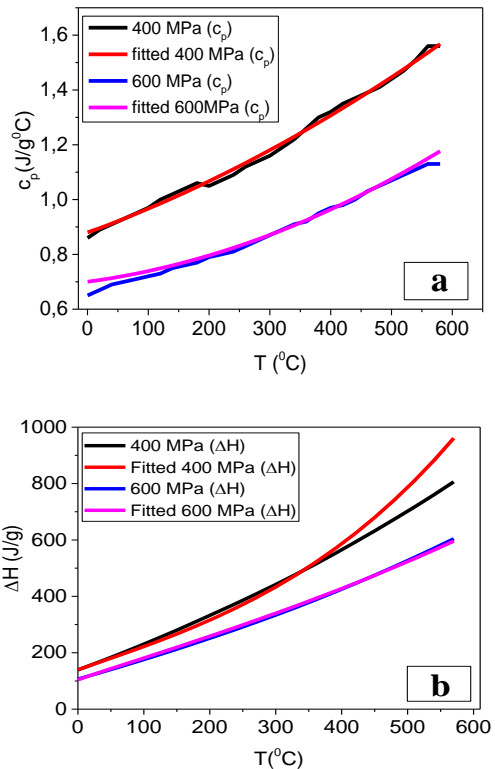


Figure 2. The Specific Heat Capacity (c_p) (a) and enthalpy (ΔH) (b) versus temperature curves of Sintered distaloy AE alloy samples with fitted c_p and ΔH values.

From Figure 2; with increasing temperature, specific heat capacity and enthalpy values of these alloys increased, but not linear increase due to increasing of atomic vibration of the alloys' chemical composition with rising temperature [20]. As pressure increased, specific heat capacity and also enthalpy values of these samples decreased. It can be recommended that decreasing of these values resulted from carbide precipitations in the microstructures of alloys. Maximum specific heat capacity and enthalpy values of these alloys have been obtained on the alloy prepared on the low pressure. (1,56 J/g°C at 580°C for specific heat capacity; 806,07 J/g at 570°C for enthalpy).

From specific heat capacity curves of distaloy AE samples; on the alloy prepared on the low pressure; appearance similar to plateau, was seen at temperature range from 200 to 380° C. It can be considered that this appearance resulted from minor precipitation formed during heat treatment [21]. At these temperatures, distaloy AE alloy gives endothermic peak. From nonlinear-squares regression values of specific heat capacity and enthalpy of distaloy AE samples on Table 3; the better fit were provided as 0,9928 on the sample prepared on the low pressure ($R^2=0,9928$) for specific heat capacity and 0,9973 on the sample prepared on the high pressure ($R^2=0,9973$) for enthalpy behaviour.

Table 1. The Specific Heat Capacity values versus temperature of sintered distaloy AE alloy samples with fitted c_p values and errors %

T (°C)	c_p (J/g°C) 400MPa	Fitted c_p (J/g°C) 400 MPa	Error (%)	c_p (J/g°C) 600 MPa	Fitted c_p (J/g°C) 600 MPa	Error (%)
0,1	0,86	0,88025513	2,35248	0,65	0,70131	7,893846154
20	0,89	0,895729145	0,643724	0,67	0,70636	5,426865672
40	0,91	0,91270368	0,297108	0,69	0,71344	3,397101449
60	0,93	0,930197752	0,021264	0,7	0,72124	3,034285714
80	0,95	0,948211362	-0,18828	0,71	0,72976	2,783098592
100	0,97	0,966744508	-0,33562	0,72	0,739	2,638888889
120	1,0	0,985797192	-1,42028	0,73	0,74896	2,597260274
140	1,02	1,005369413	-1,43437	0,75	0,75964	1,285333333
160	1,04	1,025461172	-1,39796	0,76	0,77104	1,452631579
180	1,06	1,046072467	-1,31392	0,77	0,78316	1,709090909
200	1,05	1,0672033	1,63841	0,79	0,796	0,759493671
220	1,07	1,08885367	1,762025	0,8	0,80956	1,195
240	1,09	1,111023578	1,928769	0,81	0,82384	1,708641975
260	1,12	1,133713022	1,224377	0,83	0,83884	1,065060241
280	1,14	1,156922004	1,484386	0,85	0,85456	0,536470588
300	1,16	1,180650524	1,780218	0,87	0,871	0,114942529
320	1,19	1,20489858	1,251982	0,89	0,88816	-0,20674157
340	1,22	1,229666174	0,792309	0,91	0,90604	-0,43516483
360	1,26	1,254953305	-0,40053	0,92	0,92464	0,504347826
380	1,3	1,280759973	-1,48	0,95	0,94396	-0,63578947
400	1,32	1,307086178	-0,97832	0,97	0,964	-0,61855670
420	1,35	1,333931921	-1,19023	0,98	0,98476	0,485714286
440	1,37	1,361297201	-0,63524	1,0	1,00624	0,624
460	1,39	1,389182018	-0,05885	1,03	1,02844	-0,15145631
480	1,41	1,417586373	0,538041	1,05	1,05136	0,12952381
500	1,44	1,446510264	0,452102	1,07	1,075	0,46728972
520	1,47	1,475953693	0,405013	1,09	1,09936	0,858715596
540	1,51	1,50591666	-0,27042	1,11	1,12444	1,300900901
560	1,56	1,536399163	-1,51287	1,13	1,15024	1,791150442
580	1,56	1,567401204	0,474436	1,13	1,17676	4,138053097

Table 2. The Enthalpy values versus temperature of sintered distaloy AE alloy samples with fitted ΔH values and errors %

T (°C)	ΔH (J/g) (400 MPa)	Fitted ΔH (J/g) (400 MPa)	Error (%)	ΔH (J/g) (600 MPa)	Fitted ΔH (J/g) (600 MPa)	Error (%)
0,1	139,35	139,88	0,378898	106,7	104,1	-2,4976
30	165,55	164,0555	-0,911	126,69	128,5114	1,417268
60	192,81	188,4331	-2,32279	147,41	151,0803	2,429371
90	221	213,4516	-3,53638	168,69	173,7609	2,918294
120	250,14	239,4294	-4,47338	190,51	196,607	3,101112
150	280,24	266,6853	-5,08268	212,81	219,6728	3,124081
180	311,31	295,5377	-5,33681	235,67	243,0121	3,021292
210	342,84	326,3054	-5,06723	259,15	266,6791	2,823265
240	374,96	359,3068	-4,3565	283,24	290,7276	2,575471
270	408,03	394,8607	-3,33519	308,02	315,2118	2,281564
300	442,08	433,2855	-2,02972	333,57	340,1855	1,944677
330	477,27	474,9	-0,49906	360,03	365,7029	1,551221
360	513,81	520,0226	1,194681	387,37	391,8178	1,135173
390	551,94	568,9721	2,993479	415,6	418,5844	0,712965
420	591,55	622,0669	4,905728	444,73	446,0565	0,297386
450	632,18	679,6258	6,98116	474,7	474,2883	-0,08681
480	673,65	741,9672	9,207578	505,62	503,3336	-0,45425
510	716,22	809,4099	11,51331	537,53	533,2466	-0,80327
540	760,26	882,2723	13,82933	570,39	564,0811	-1,11844
570	806,07	960,8732	16,11068	604,06	595,8913	-1,37084

Table 3. The fit coefficients and nonlinear –squares regression values of specific heat capacity and enthalpy behaviours of distaloy AE samples

	c_p		ΔH	
	Distaloy AE 400 MPa	Distaloy AE 600 MPa	Distaloy AE 400 MPa	Distaloy AE 600 MPa
c_0	0,87927415	0,7	0,8000184	0,750018
c_1	0,00080976	0,0003	0,000004	0,000004
c_2	6,4942E-07	0,0000009	0,0000059	0,000001
c_3	0,0000009	0,0000001	0,00008	0,00079
c_4	-	-	-140	-106
R^2	0,9928	0,9750	0,9652	0,9973

In Figure 3; The SEM images and EDS spectrums of sintered distaloy AE samples are given. From Figure 3; Surface appearances of both of distaloy AE samples, have smooth surfaces. With increasing pressure; porosity closed, grain binding and grain boundaries occurs. It was considered that porosity existence has an increasing effect on the thermophysical properties due to easily dissipating of heat in porous structures. According to EDS spectrums of sintered distaloy AE samples; it was observed that with increasing of pressure; C, Ni, Cu ratios in the microstructure of alloy decreased, ratios of Fe and Mo alloying elements increased. This case is also observed on the XRD patterns of these distaloy AE samples (seen in Figure 4).

According to literature; on the sintering at high temperatures (1200°C in this study), liquid phase occurs from reaction between distaloy AE matrix and carbide precipitates and provides densification

of structures of these alloys [22]. From EDS spectrums in Figure 3 (c) and (d), carbon amounts on the microstructures of the distaloy AE alloys prepared on the 400 MPa pressures has more than that of other distaloy AE alloys; more carbon amounts leads Cu-rich- martensitic transformation [23]. Besides martensitic structure into the distaloy AE alloy samples, porosity existence plays a role on the thermophysical properties of these samples. During sintering process; Cu melts at almost 1085°C temperature and into the Cu melts Ni alloying element diffuses. Martensitic structure having Ni and Cu rich possesses a strengthening structure [23]. It can be considered that besides porosity existence and martensitic structure on the microstructure of the distaloy AE alloy prepared on the low pressure has a role on the increasing of the specific heat capacity and enthalpy properties.

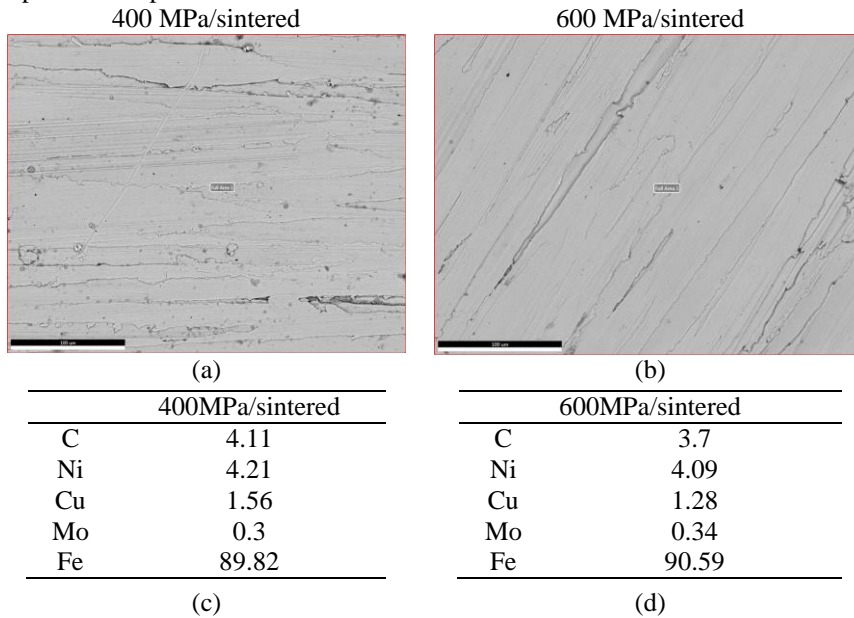


Figure 3. The SEM images (a and b) and EDS Spectrums (c and d) of distaloy AE compacts prepared on the 400 and 600MPa pressures

In Figure 4.; the XRD patterns of crystal structures of powder and sintered distaloy AE samples are given. From Figure 4. It was observed that Fe and Ni alloying elements into the microstructures of distaloy AE samples have higher intensity peaks than other alloying elements such as Cu. On the

XRD pattern of distaloy AE powder; at 43.4° diffraction angle (111) cubic crystal structure varies to (011) cubic crystal structure on the XRD patterns of both of sintered alloys at diffraction angle range from 50.59- 51.85°.

Also, peaks of Cu, Ni having (020) cubic crystal structure on the XRD pattern of distalloy AE powder is not seen on the XRD patterns of both of sintered distalloy AE samples.

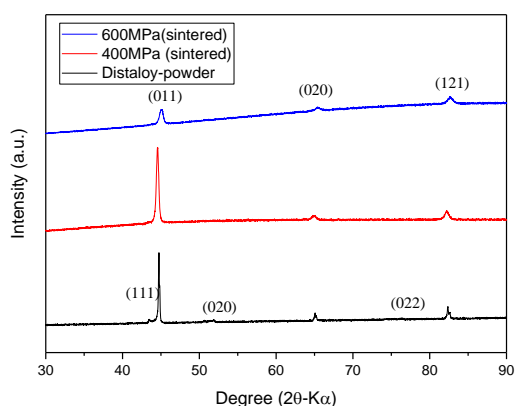


Figure 4. The XRD patterns of powder and sintered Distalloy AE alloy samples

Conclusion

On this work; specific heat capacity and enthalpy behaviours of distalloy AE alloy samples prepared by powder metallurgy method were examined. Following experimental results are given;

- The specific heat capacity and enthalpy values of both of Distalloy AE samples increase with increasing temperature.
- The pressure has a negative effect on the specific heat capacity and enthalpy, increasing the pressure results in decreasing the specific heat capacity and enthalpy value of distalloy AE alloys.
- It can be considered that existences of martensite structure porosity existence in the microstructures of distalloy AE results in reduction of thermophysical properties with respect to pressure increase.

Acknowledgement:

The authors are greatly thankful to Cukurova University research funding (FBA-2018-11074)

References

1. E. Morintale, A. Harabor, C. Constantinescu, P. Rotaru, Use of heat flows from DSC curve for calculaion of specific heat of the solid Materials, *Physics AUC.*, **2015**, Vol. 23, pp. 89-94
2. E. Wielgosz, T. Kargul, J. Falkus, Comparison of experimental and numerically calculated thermal properties of steels, *International Conference on Metallurgy and Materials, Metal* **2014**, May 21 st-23rd 2014, Brno, Czech Republic
3. H.Fang, M.B. Wong, Y. Bai 2015, Use of kinetic model for thermal properties of steel at high temperatures, *Australian Journal of Civil Engineering*, **2015**, Vol.13:1, pp.40-47,
4. K.K. Kelley, High-temperature heat-content, heat-capacity, and entropy data for inorganic

compounds, *Bureau of Mines Bulletin* **1949**, Vol.476, pp.192.

5. H.Abdoos, H. Khorsand, A.R. Shahani, Fatigue behaviour of diffusion bonded powder metallurgy steel with heterogeneous microstructure, *Materials and Design*, **2009**, Vol.30 pp. 1026–1031
6. W.B.James, R.C. OtBrien, High performance Ferrous PM Materials: The Effect of Alloying Method on Dynamic Properties. *Progress in powder Metallurgy*. Princeton NJ: MPIF; 1986.
7. L.Alzati, A. Bergmark, J. Andersson, Fatigue performance of PM steel in assintered state. Presented at PMAI conference, Mumbai, India, February; **2005**
8. P.Lindskog, The history of distalloy, *Powder Metallurgy*, **2013**, 56:5, pp.351-361,
9. K.E.Öksüz, L.C. Kumruoğlu, O. Tur, Effect of Sic_p on the microstructure and mechanical properties of sintered Distalloy DC composites, (5th International Biennial Conference on Ultrafine Grained and Nanostructured Materials, UFGNSM15), 11-12 November 2015, Tehran-Iran, *Procedia Materials Science*, **2015**, Vol.11, pp.49 – 54
10. S.S. Panda, V. Singh, A.Upadhyaya, D. Agrawal, Sintering response of austenitic (316L) and ferritic (434L) stainless steel consolidated in conventional and microwave furnaces, *Scripta Materialia*, **2006**, Vol.54 pp.2179–2183
11. S.Giménez, A. Vagnon, D. Bouvard D., O.van der Biest, influence of the green density on the dewaxing behaviour of uniaxially pressed powder compacts, *Materials Science and Engineering A*, **2006**, Vol.430, pp.277–284
12. R.Yılmaz,,M.R.Ekici M.R., Üretim parametrelerin düşük alaşımlı TM çeliklerin sertlik ve aşınma özelliklerine etkisi *ISITES2015 Valencia –Spain*, pp.2545-2554
13. K. Zarebski, P. Putyra, 2015, Iron powder-based graded products sintered by conventional method and by SPS, *Advanced Powder Technology*, **2015**, Vol. 26, pp.401–408
14. H.A.Al-Qureshi, Galiotto A., Klein A.N., On the mechanics of cold die compaction for powder metallurgy, *Journal of Materials Processing Technology*, **2005**, Vol. 166, pp.135–143
15. A.N. Acar, A.K. Ekşi, A. Ekicibil, Effect of pressure on the magnetic and structural properties of X2CrNiMo17-12-2 austenitic stainless steel prepared by powder metallurgy method *Journal of Molecular Structure*, **2019**, Vol. 1198, 126876 page:12
16. A.N. Acar, R.N. Mutlu, A.K. Ekşi, A. Ekicibil, B.Yazıcı, Effect of temperature and pressure on mechanical, surface and electrochemical properties of Al-1.5Cu-5.5Zn-2.5Mg (Alumix-431), *Anti-Corrosion Methods and Materials*, **2018**, Vol. 65/6, pp.558–571

17. S. Butković, M. Oruč, E.Šarić, M., Mehmedović M., Effect of sintering parameters on the density, microstructure and mechanical properties of the niobium-modified heat-resistant stainless steel GX40CrNi25-20 produced by MIM technology, *Materiali in tehnologije / Materials and technology*, **2012**, 46, 2, 185–190,
18. S. Pandya, K.S. Ramakrishna, A.R. Annamalai, A. Upadhyaya, Effect of sintering temperature on the mechanical and electrochemical properties of austenitic stainless steel, *Materials Science and Engineering A*, **2012**, 556, pp.271–277,
19. S. Butković, Sinterability and tensile properties of nickel free austenitic stainless steel X15CrMnMoN 17 11 3, *Tehnički vjesnik*, **2013**, 20, 2, pp.269-274, (*Technical Gazette* **2013**, 20, 2, pp.269-274).
20. B. Karthikeyan, S. Ramanathan, V. Ramakrishnan, A calorimetry study of 7075Al/SiC_p composites, *Materials and Design*, **2010**, Vol. 31 pp. S92-S95.
21. B. Witthan, H. Reschab, R. Tanzer, W. Shützenhöfer, G. Pörtlacher, Thermophysical properties of chromium-nickel-molybdenum steel in the solid and liquid phases, *International Journal of Thermophysics* **2008** 29:434-444
22. J. Karwan-Baczewska, Processing and properties of distalloy SA sintered alloys with boron and carbon, *Archives of Metallurgy and Materials* **2015**, 60 (1), pp.41-45
23. H. Abdoos, H. Khorsand, A.R. Shahani, Fatigue behavior of diffusion bonded powder metallurgy steel with heterogeneous microstructure, *Materials and Design*, **2009**, Vol. 30, pp.1026–1031